Dipole–dipole plasmon interactions in self-assembly of gold organosol induced by glutathione

Soumen Basu, Sudipa Panigrahi, Snigdhamayee Praharaj, Sujit Kumar Ghosh, Surojit Pande, Subhra Jana and Tarasankar Pal*

Received (in Durham, UK) 25th May 2006, Accepted 20th July 2006
First published as an Advance Article on the web 10th August 2006
DOI: 10.1039/b607399a

Assemblies of gold nanoparticles in an organic medium have been synthesized to study the plasmon–plasmon interactions amongst the gold nanoparticles. A pH-sensitive biomolecule, glutathione (GSH), has been introduced as a molecular linker of the 'parent' gold nanoparticles to obtain small nanoparticle aggregates. The optical spectra of gold nanoparticles shifted to the red region indicate dipole–dipole interactions in the gold particle assembly. The aggregates have been characterized by UV-Vis, FTIR, HRTEM and XRD techniques. A controlled method of aggregating gold nanoparticles in organic solvents has been achieved successfully under controlled pH conditions with different concentrations of the molecular linker, GSH. The pH dependent anchoring of GSH onto gold surfaces has been proved beyond doubt to bring about nanoparticle aggregation.

Introduction

Bottom-up assembly of inorganic nanoparticles is a promising means of creating advanced materials with superior electronic, optical, and mechanical properties.[1,2] Due to the spherical symmetry and uniform reactivity of individual nanoparticle surfaces, the synthesis of small controlled nanoparticle assemblies is a significant challenge. Recently, assembling individual nanoparticles into ensembles of specific shape and structure has become a widely pursued objective.[3] The organization and patterning of inorganic nanoparticles into 2D and 3D functional structures is a fundamental prerequisite for the assembly of chemical, optical, magnetic, and electronic devices.[4] Several approaches have been described for the generation of 2D and 3D arrays of metal and semiconductor nanoparticles: (i) by evaporation of the solvent of hydrophobic colloids,[5] (ii) by random inclusion of the nanoparticles into gel and glassy matrices,[6] (iii) by template-mediated synthesis at structured surfaces in porous protein crystals[7] or in bacterial superstructures, and (iv) through chemical coupling in solution by means of bifunctional cross-linkers.[8,9] An example of the latter is the alkanedithiol-directed aggregation of gold nanoparticles.[8,9] The aggregation of nanoparticles induced by specific biological agents has attracted significant interest as a self-assembly process for the construction of complex nanostructures that exhibit new collective properties. It is interesting to generate and study the interparticle interactions in a closely packed assembly of metal nanoparticles while the particles are held by weak forces.

With their excellent compatibility with biomolecules[10–13] and distance-dependent optical absorbance,[10,14] colloidal gold nanoparticles have attracted intense scientific and technological interest. Metallic particles of gold in the nanometre size regime exhibit a strong absorption band in the visible region and this is indeed a small particle effect, since it is absent in the individual atoms as well as in the bulk.[15,16] The physical origin of the light absorption by metal nanoparticles is the coherent oscillation of the conduction band electrons induced by the interacting electromagnetic field. The absorption band results when the incident photon frequency is resonant with the collective oscillation of the conduction band electrons and is known as the surface plasmon resonance (SPR). The resonance frequency of this SPR is strongly dependent upon the size, shape, dielectric properties and local environment of the nanoparticles.[15,17–21] When a cluster of metal nanoparticles are placed in close proximity to one another, the interparticle coupling effects become very important in studying the particle plasmon resonances, especially the shift of the plasmon resonant wavelength as a function of particle separation. In colloidal solutions, the color of Au nanoparticles may range from red to purple, to blue and almost black, due to the formation of aggregates. Nanoparticle aggregates of gold with interparticle distances substantially greater than the average particle diameter appear red (with $\lambda_{max} \approx 520$ nm), but as the interparticle distances in the aggregates decrease to less than approximately the average particle diameter, the color becomes blue.[22–24]

The recent development of nanoscience and nanotechnology involves the synthesis and stabilization of metal nanoparticles in non-aqueous solvent.[25–27] The organic solution-based synthesis of metallic nanoparticles possesses certain advantages. It shows a high degree of control over the nanoparticle size, monodispersity and chemical nature of the nanoparticle surface. These metal organosols are convenient objects for the investigation of the physicochemical properties of metallic nanoparticles.[28] Moreover, a wide number of reactions are catalyzed in organic media. Nanoparticles in organic media are becoming an interesting topic in view of their various applications in optical devices,[29,30] optical energy

Department of Chemistry, Indian Institute of Technology, Kharagpur, 721302, India. E-mail: tpal@chem.iitkgp.ernet.in

transport,[31,32] near-field scanning optical microscopy (NSOM),[33,34] surface enhanced Raman scattering spectroscopy,[35,36] chemical and biological sensors.[14,37] The properties of regularly packed aggregates have been well explored.[38] The interesting colors observed in gold sols have led to extensive study of their optical spectroscopic properties in an effort to correlate their behavior under different microenvironmental conditions. Without the application of organosol systems, the study often fails to register the impacts of the solvent on the sol properties. However, regularly packed aggregates have variable optical properties. If these properties can be controlled, then there might, for example, be applications for the clusters as the substrates in SERS, as novel pigments or in spectrally selective coatings for solar glazing.[39] Unfortunately, in general when gold nanoparticles in suspension are aggregated or densified, they precipitate out as mesoporous sponges, losing their plasmon resonance in the process. Kimura *et al*. have reported the formation of a three dimensional superlattice of gold nanoparticles.[40] The groups of Mirkin[37] and Alivisatos[41] have demonstrated the formation of aggregated metal clusters, using DNA as the recognition element in aqueous medium. Some of the amino acids can induce aggregation of gold nanoparticles.[42] Mandal *et al*. have reported the aggregation of cysteine-capped silver particles.[43]

In this paper, we report a simple method for the formation of gold aggregates in organic solvents *i.e*., aggregation of a Au organosol by the modification of gold nanoparticles with pH sensitive and ionizable thiols, namely, glutathione (GSH) which is used as a short chain molecular linker because of its biological and clinical significance. High-resolution transmission electron microscopy (HRTEM), X-ray diffraction (XRD), Fourier transform infrared spectroscopy (FTIR) and absorption spectroscopy have been used to characterize the assemblies. It has been found that these nanocrystals self-assemble into monolayers or multilayers after the ligand-exchange process. The particle size, interparticle distances and absorption band wavelengths are found to be highly dependent on the pH of the medium and the concentration of the GSH.

Experimental

Reagents and instruments

All the reagents used were of AR grade and the solvents were dried. Chloroauric acid ($HAuCl_4 \cdot 3H_2O$) was purchased from Aldrich. Sodium borohydride (Aldrich) and glutathione (Aldrich) were used as received.

The absorption spectrum of each solution was recorded in a Spectrascan UV 2600 digital spectrophotometer (Chemito, India) in a 1 cm well-stoppered quartz cuvette. The spectra were taken with reference to a solvent in a reference cell in the double beam spectrophotometer to subtract solvent background. HRTEM was carried out on a JEOL JEM-2010 UHR transmission electron microscope. Samples were prepared by placing a drop of solution on a carbon coated copper grid. FTIR Spectral characteristics of the samples were collected in reflectance mode with Nexus 870 Thermo-Nicolet instrument coupled with a Thermo-Nicolet Continuum FTIR Microscope. One drop of the test solution was placed on a KBr pellet and was dried under vacuum for 6 h before analysis. The X-ray diffraction (XRD) pattern was recorded in an X'pert pro diffractometer with Co (K_α = 1.78 891) radiation.

Synthesis of gold nanoparticles

Gold nanoparticles capped with tetraoctylammonium bromide (TOAB) in toluene were prepared using the biphasic reduction procedure. An aqueous solution of chloroauric acid (5 mL, 2.0 mM) was first extracted into toluene using the phase transfer catalyst, TOAB (5 mL, 2.0 mM). Addition of phase transfer reagent to the aqueous phase resulted in swift movement of the $AuCl_4^-$ ions to the organic layer. The solution was diluted by the addition of 15 mL of toluene. Finally, 2 mg of sodium borohydride was introduced and the reaction mixture was shaken vigorously. During shaking, at first, the yellow color of $AuCl_4^-$ was found to disappear and the solution became colorless. Then, the solution slowly turned red to wine red, indicating the formation of gold nanoparticles. After that the sol showed no further change in color implying the completion of the reaction. The final concentration of gold in this experiment was 0.5 mM. The organosol prepared by the above method was evaporated to *ca*. 2 ml in a rotary evaporator resulting in a gold concentration of 5 mM. An aliquot of 30 μL of this highly concentrated gold suspension was diluted to 3 mL with THF.

Making glutathione–Au assemblies

In a typical synthesis, to an aliquot of colloidal gold (3 mL, 50 μM) dispersed in THF, dilute HCl (100 μL, 10 mM) was added to lower the pH value. Then, an aliquot of GSH solution (30 μL, 10 mM) prepared in THF was added to that deep red acidic gold colloidal solution. The color changed from red to blue indicating the formation of the aggregates of gold nanoparticles. The method is reproducible and the gold nanoparticle aggregates in organic solvent prepared by this method remain stable for a few days.

Results and discussion

The formation of gold nanoparticle aggregates was probed by monitoring the absorption changes at several stages of the reaction. Fig. 1 shows the absorption spectral features for the evolution of gold aggregates in THF. The aqueous solution of $AuCl_4^-$ ions exhibits an absorption peak at 293 nm (trace a) which can be attributed to the metal-to-ligand charge transfer (MLCT) band of $AuCl_4^-$ complexes.[44] The toluenic dispersion of TOAB shows no characteristic absorption maximum in the range of 300–700 nm (trace b). Addition of the toluenic solution of TOAB to the aqueous solution of $HAuCl_4$ caused the disappearance of the 293 nm absorption band due to $AuCl_4^-$ complexes and a new absorption band appears with a shoulder at 345 nm (trace c) which can be ascribed to the formation of an ion-pair $[TOA]^+[AuCl_4]^-$, ($[TOA]^+$ = tetraoctylammonium ion).[44] Upon addition of $NaBH_4$ to the reaction mixture, the yellow color of the solution gradually disappeared and after a certain time, the solution became completely colorless, indicating the formation of AuO_2^-

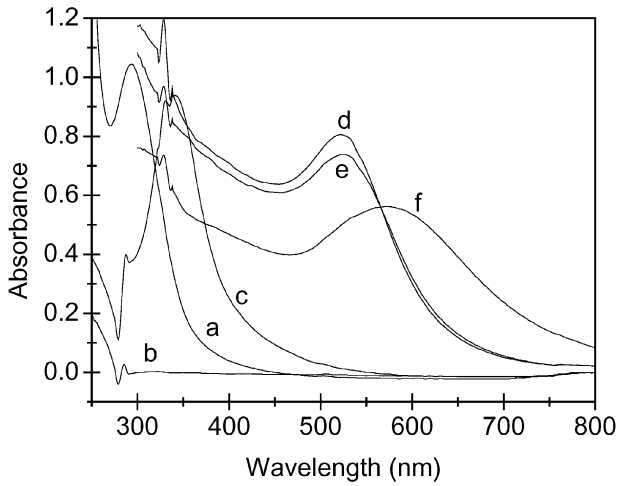

Fig. 1 Absorption spectra of (a) aqueous solution of $HAuCl_4$, (b) the toluenic dispersion of TOAB, (c) $[TOA]^+[AuCl_4]^-$, (d) TOAB-capped gold nanoparticles in toluene, (e) TOAB-capped gold nanoparticles in THF and (f) gold aggregates in THF induced by GSH at pH $\approx$ 4.

species in the alkaline condition.[45] On further shaking, the appearance of a pinkish tinge within the solution indicates the onset of the evolution of gold particles. The color of the solution gradually changed from light pink to red to wine red upon completion of the reaction. Absorption measurement of this resulting solution shows a new absorption band with maximum at 530 nm (trace d), which corresponds to a typical plasmon band of gold nanoparticles. The metallic particles dispersed in toluene were dried under vacuum and redispersed well in tetrahydrofuran (THF) without any sign of aggregation or precipitation of the particles. Trace e shows the surface plasmon resonance with a maximum at 521 nm of gold nanoparticles dispersed in THF. The blue shift of the SPR on changing the solvent from toluene to THF is due to the change in refractive index of the medium.[46] Upon addition of GSH solution to the deep red solution of colloidal gold followed by acidification with dilute HCl, the color of the solution changed from red to blue. Absorption measurement of this blue solution shows a red-shifted broad band with a maximum at $\sim$580 nm with an observable decrease in the absorption intensity (trace f). It is now well documented in the literature that the assembly of nanoparticles in various states of aggregation influences the plasmon resonance.[15] The appearance of an absorption maximum at $\sim$580 nm indicates that the particles are assembled into an aggregated structure. This is attributable to electric dipole–dipole interactions and coupling between plasmons of neighboring particles in the aggregates.

The optical properties of small particles in the nanometre size range are mainly determined by two contributions:[47] (i) the particles acting individually as an isolated sample and (ii) the collective properties of the whole ensemble. But in the closely packed aggregates of an ensemble of a large number of particles (as seen in the present case), the isolated-particle approximation breaks down and electromagnetic interactions between the particles become important and affect the surface plasmon resonance enormously. This effect is negligible if $D > 5r$, where D is the center-to-center distance and r the radius of the particles, but is increasingly important when D is less than that. Therefore, in the aggregates of gold nanoparticles, it is very difficult to observe the properties of the isolated sample as interparticle interactions generally overpower the single-particle property. The color of the solution in such aggregates depends on nanoparticle spacing. Nanoparticle aggregates of gold with interparticle distances substantially greater than the average particle diameter appear red with $\lambda_{max} \approx 520$ nm, but as the interparticle distances in the aggregates decrease to less than approximately the average particle diameter, the color becomes blue. The blue color of the solution in the present case indicates that the interparticle distances in the aggregate are obviously less than the average particle diameter, which is also evident from the TEM studies. The appearance of a red-shifted band at $\sim$580 nm can be attributed to the surface plasmon resonance of gold organized into an aggregated structure.

We have studied the aggregation of gold organosol with GSH (containing α-NH_2 and -SH groups) in THF for the first time. The applicability of cysteine (cys) was also tested as the molecules possess similar functional groups to GSH. It was seen that both the aggregating species are able to interlink gold nanoparticles in THF shortening the interparticle distance. Thus, the 'field effect' becomes effective as a result of which a broad banded peak in the red region is observed. Between the two aggregating species, cys has shown to be very effective and prompt in its action. This was confirmed from the ready appearance of the 580 nm peak (Fig. 2, trace c). This peak was also observed when GSH was introduced into the system under identical conditions (temperature, concentration and pH of the medium) (Fig. 2, trace b). The spectral change (aggregation) is detectable with a lower concentration of cys (5 μM) than GSH. To confirm the aggregating behavior of GSH and cys, we have separately considered the action of 1-dodecanethiol (1-DDT) on the gold organosol in THF. The stabilizing action of DDT is well documented in literature but

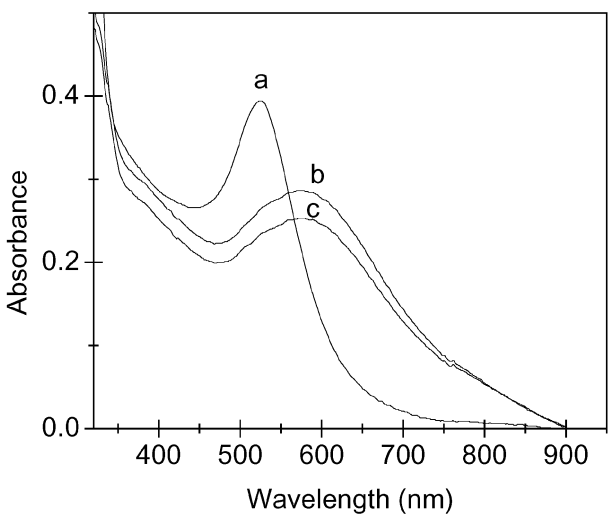

Fig. 2 Absorption spectra of (a) 1-DDT capped gold nanoparticles in THF, (b) gold aggregates in THF induced by GSH and (c) gold aggregates in THF induced by cysteine at pH $\approx$ 4.

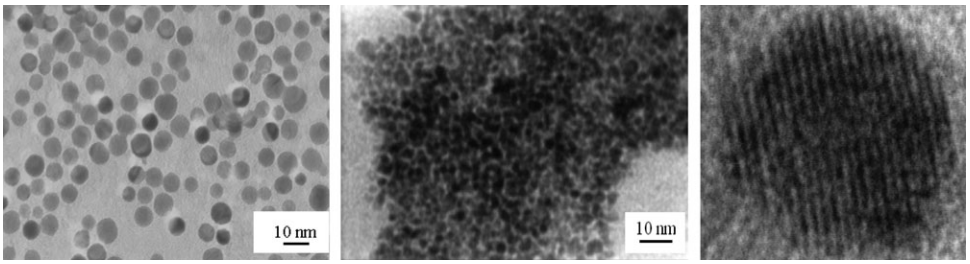

Fig. 3 Transmission electron micrographs of (A) gold particles dispersed in THF, (B) aggregates of the parent particles after addition of GSH and (C) high-resolution transmission electron micrographs of an individual GSH capped gold nanocrystal.

its monofunctionality does not allow it to interlink the gold nanoparticles in question. Hence, no aggregation was detected; only a slight shift (~2 nm) of λ_{max} value was noted (Fig. 2, trace a).

Fig. 3 shows the transmission electron micrographs of the (A) TOAB-capped gold particles dispersed in THF, (B) aggregates of the parent particles after addition of GSH at pH ~ 4 and (C) high-resolution transmission electron micrographs of an individual GSH capped gold nanocrystal. The TOAB-capped gold colloids produce nearly spherical particles with diameter ranging from 5 to 6 nm which is shown in Fig. 3A. From the Fig. 3B, it is seen that the spherical and tiny gold particles with a mean diameter of ~ 6 nm undergo coalescence and form a closely packed assembly. In a HRTEM image of Au-GSH nanocrystals (Fig. 3C), the particles show lattice images originating from a single crystal. The distances between the adjacent lattice fringes, measured as 2.36 Å, are the interplanar distances of the Au {111} plane, which are in excellent agreement with the {111} *d*-spacing of bulk Au (2.355 Å).

The XRD pattern for the GSH-capped gold aggregates is shown in Fig. 4. Several peaks are observed, these being at 44.2°, 51.5°, 76.4°, 93.3° and 98.6°, which correspond to the {111}, {200}, {220}, {311} and {222} facets of the fcc crystal structure of gold, respectively. The observation of diffraction peaks of gold nanoparticles indicates that these are crystalline in nature. The broadening of the spectrum is related to the reduced particle size.

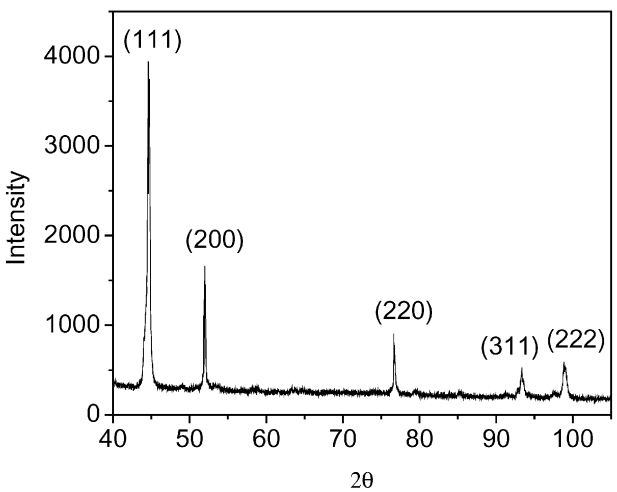

Fig. 4 X-Ray diffraction pattern of gold aggregates.

In a preliminary control experiment, we observed the optical spectra of a TOAB capped gold colloid in THF and then the effect of sequential addition of 10 mM HCl solution in the organosol system. There is almost no shift in the peak position until the pH value is lowered to ~3.5, indicating no aggregation effects from the added HCl solution. At still lower pH the particles aggregate due to the decrease in energy barrier by both lowering the surface potential of the particles and increasing the ionic strength. The evolution of particle aggregates due to the addition of glutathione is dependent on the pH of the sol system. Generation of aggregates with a perfect blue color is observed at pH $\leq$ 5 with glutathione. The molecular structure of GSH is shown in Scheme 1. Glutathione is the major cellular antioxidant that plays a crucial role in maintaining the balance between oxidation and antioxidation. This tripeptide also plays an important part in cellular detoxification and is required for many aspects of immune response. It is also an important factor in brain damage,[48] glucose homeostasis,[49] HIV expression[50] and cancer therapy.[51] As glutathione consists of amino acids *viz*. glutamic acid, cysteine and glycine, its binding mode with gold surfaces is pH sensitive. In GSH, several possible binding points are present, which gives it different binding possibilities with gold. The availability of one or several anchoring points for binding on the gold surface depends primarily on the pH of the medium. Some of the anchoring points in glutathione are the two carboxylic groups in the glutamic acid moiety and glycine residue, three $-NH_2$ groups in the three amino acids and the sulfur atom in the cysteine residue. The pK_a values corresponding to the two carboxylic groups have been determined as 2.56 and 3.50[52] and for the cysteine residue as 9.42

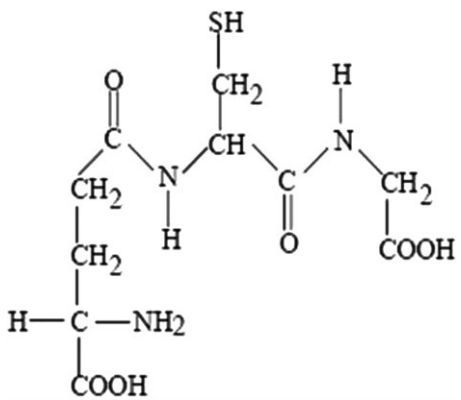

Scheme 1 Molecular structure of glutathione (GSH).

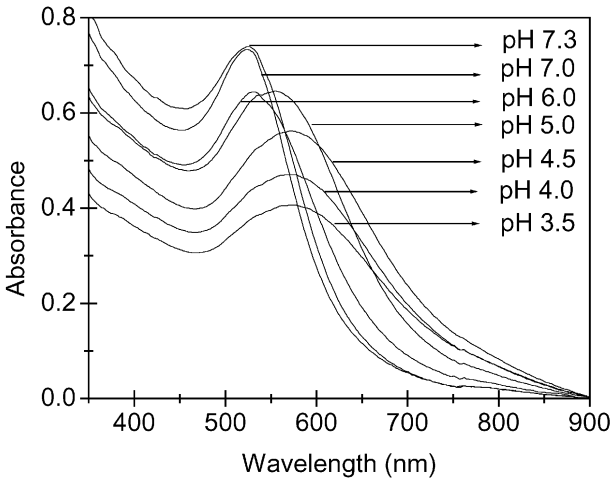

Fig. 5 UV-visible spectra of gold aggregates in THF at various pH.

for aqueous solutions.[53] However, predicting solely from the pK_a values of the different groups as to which binding mode is expected is not always accurate since the acid–base character of a certain group can change the binding capability with the metal surface and the medium.[54] It is to be mentioned that in organosol systems, gold is stabilized sterically. The GSH binds with the gold surfaces through –SH as well as $–NH_2$ anchoring points and hence the gold particle aggregates. At lower pH, linking *via* the α-amines is activated due to the zwitterionic species, but linking through –COOH groups is suppressed due to the undissociated carboxylic groups. However, at intermediate or higher pH, dissociation of the carboxyl group would be expected to hinder the binding of gold colloids *via* the α-amine group, resulting in little or no cross-linking. Fig. 5 shows the optical spectra of gold colloids (50 μM) in THF at different pH for a particular concentration of GSH solution (0.1 mM). There is clearly a progressive new color development for the organosol system in THF and red shifting of the surface plasmon resonance band with decreasing pH is observed. At pH ≈ 7, no spectral changes occur but as the pH decreases then the dipole plasmon resonance shifts to the longer wavelength. At lower pH, one –SH group of the cysteine moiety and the primary $–NH_2$ group of the glutamic acid moiety can bind effectively the gold nanoparticles to form aggregates which is authenticated from FTIR spectra. It should be mentioned that in an organic solvent like THF exact measurement of pH is not possible, and therefore an average pH value has been given. In this regard, because of the delocalization of electrons, the other two –NH– moieties of GSH remain ineffective. The surface coordination of the gold particles with GSH was also accomplished from the FTIR spectrum. Fig. 6A shows the FTIR spectrum recorded from the gold aggregates in the spectral window 2400–2600 cm^{-1} (curve 1) along with the spectrum recorded from GSH powder (curve 2) at pH ≈ 4. The prominent –SH vibrational band centered at *ca.* 2524 cm^{-1} is clearly seen in the free GSH molecules (curve 2) and vanishes upon coordination with colloidal gold (curve 1). Further evidence for the presence of surface bound GSH is provided by FTIR measurements of the gold particles in the spectral window 3200–3500 cm^{-1} (curve 1, Fig. 6B). The N–H stretch of the GSH molecules is observed at 3250 cm^{-1} (curve 2, Fig 6B). But a weak and red shifted (3307 cm^{-1}) peak position (curve 1, Fig. 6B) suggests an interaction of the N–H group with the gold particles. The position of the carboxylate stretching vibration in the GSH capped gold remains unaltered (curve 1, Fig. 6C) at 1713 cm^{-1} which suggests that there is no hydrogen bonding.

The classical Derjaguin–Laudau–Verwey–Overbeck (DLVO) theory[55] has been widely employed in colloid science to study particle–particle interactions, colloidal stability, coagulation and the behavior of the electrolyte solutions. This theory is based on the idea that pair-wise interaction forces dominate which arise from the interplay of attractive van der Waals forces, F_{attr} and repulsive Coulomb forces, F_{rep} screened by Debye–Hückel ion clouds. Obviously, the dispersed colloid is stable for $F_{rep} \gg F_{attr}$ whereas the condition of $F_{rep} \ll F_{attr}$ leads to aggregation. Therefore, in colloidal solution several factors, such as particle size, surface potential, and electric double layer influence the stability of nanoparticles and their aggregation. Nanoparticles are stable in solution due to electrostatic repulsion of their charged surface. Lack of sufficient surface charge or stabilizing agent will cause the particles to aggregate or precipitate. In the present experiment, tetraoctylammonium ions are adsorbed onto the surface of gold nanoparticles, creating a surface charge that stabilizes the particles. Addition of glutathione to the TOAB-stabilized gold nanoparticles disrupts the tetraoctylammonium ionic layers causing particle aggregation *via* slow 'place exchange reaction'. Since there are no species in solution to generate sufficient surface charge on the gold particles, the particles will aggregate. Thus, the density of the surface charge and the surface potential of the particles can be varied over a wide range. When the surface potential is far away from the

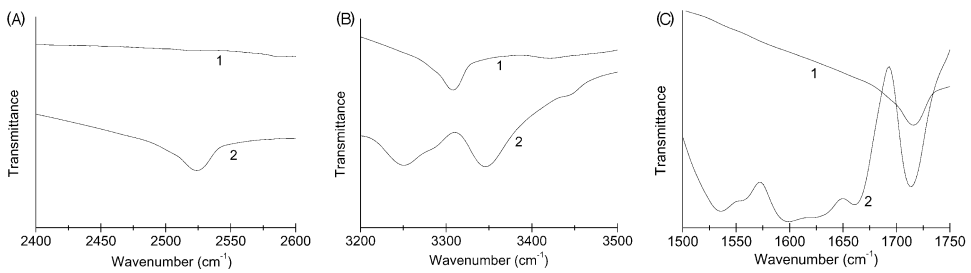

Fig. 6 FTIR spectra of pure glutathione (curve 2) and glutathione induced gold aggregates (curve 1) at pH ≈ 4 in the spectral windows (A) 2400–2600 cm^{-1}, (B) 3200–3500 cm^{-1} and (C) 1500–1750 cm^{-1}.

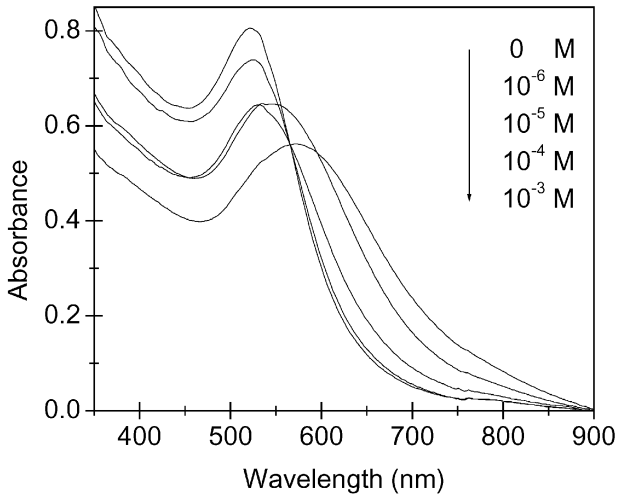

Fig. 7 UV-visible spectra for gold aggregates at different concentration of glutathione at pH ≈ 4.

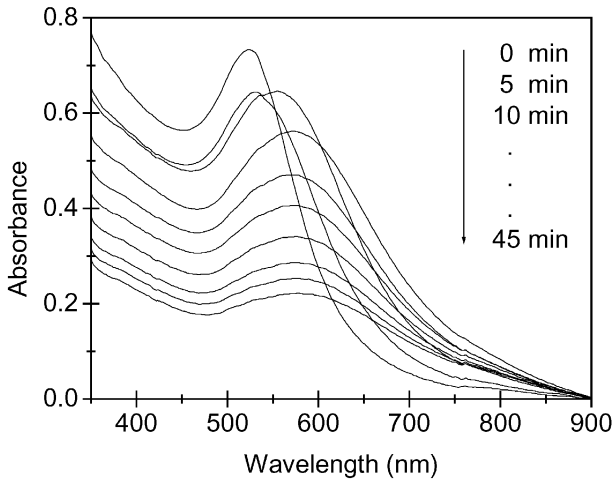

Fig. 8 Time-dependent UV-visible spectra of gold nanoparticles at pH ≈ 4 recorded at various times after addition of glutathione (0.1 mM).

potential of zero charge (pzc), the particles are highly dispersed and very stable; when the surface potential is near or equal to the pzc and the electrostatic repulsion cannot overcome the van der Waals attraction, the nanoparticles become aggregated. Upon addition of glutathione to a solution of colloidal gold, one functional group reacts with the gold nanoparticles while the other functional groups remain extended from the nanoparticles. Thus, the multifunctional linker molecules position the colloidal nanoparticles in close proximity to each other, causing aggregation between the particles.

In the present experiment, the TOAB molecules present on the particle surface provide a steric barrier against aggregation. The thickness of the electrical double layer is characterized by the inverse of Debye length (κ^{-1}). For a symmetric ($\nu : \nu$) electrolyte, the inverse Debye length is given by

$$\kappa^{-1} = \sqrt{\frac{2000 e^2 \nu^2 N_A M}{\varepsilon k_B T}}$$

For this study, the system temperature is assumed to be T = 298 K, and the permittivity of toluene at this temperature is $\sim 2.39 \times 10^{-10}$ C^2 N^{-1} m^{-2}. The remaining constants in the expression for the inverse Debye length are the Boltzmann constant, $k_B = 1.381 \times 10^{-23}$ J K^{-1}, the fundamental electron charge, $e = 1.602 \times 10^{-19}$ C and Avogadro number, $N_A = 6.022 \times 10^{23}$ mol^{-1}. Since the electrolyte concentration (c) of the colloidal solution is kept at millimolar (0.1 mM) level, the inverse Debye length is calculated as 1.78×10^7 which indicates that the electrical double layer surrounding the colloidal particles is large enough to be treated as a constant. So the surface potential becomes the determining factor for the stability of the nanoparticles. Upon addition of GSH molecules to the gold colloid, the particle surface becomes neutral leading to the aggregation of the gold particles.

To evaluate the morphological effect on the ligand (GSH) concentration, a set of gold aggregates was prepared by using GSH at pH ≈ 4 with variable molar ratios of [GSH]/[Au(0)] from 0 to 20. The optical spectra of these aggregates are shown in Fig. 7. For the sample with a very low GSH content, *i.e.*, [GSH]/[Au(0)] = 0.02, no assembly is observed. When we increased GSH concentration, the λ_{max} shifted to higher wavelength region, resulting a change in the morphology from isolated domains to compact domains.

Large gold nanoparticles (>5 nm) exhibit a surface plasmon resonance (SPR) that is based on the size of the metal core and the interparticle spacing (dipolar coupling) between the nanoparticles. We have monitored the shift in the surface plasmon resonance of gold nanoparticles as a function of time to investigate the kinetics of the aggregation process. A solution of GSH was added to the acidic solution (pH ≈ 4) of gold particles at room temperature and the spectra were acquired over different time intervals as shown in Fig. 8. A distinctive red shift of the dipole plasmon resonance from 520 to 580 nm is observed which indicates that interparticle spacing decreases with the progress of the place exchange reaction.

Conclusion

We have demonstrated a very simple approach for preparing gold nanoparticle aggregates by linking individual gold colloidal particles in a dispersion. The treatment of TOAB-stabilized gold nanoparticles with GSH molecules causes their aggregation. It is possible to control the interparticle distance in the self-assembled gold nanocrystals over a limited range by capping with GSH. Upon aggregation, the solution shows a broad red shifted absorption band around 580 nm, which is attributed to interparticle plasmon coupling between the particles. The degree of coupling, and thus the nature of this band, are influenced by the pH of the colloidal solution and the concentration of GSH solution. From the FTIR spectra it was confirmed that GSH binds to the gold surface *via* a strong thiolate bond whereas the $-NH_2$ group coordinates with the gold surface weakly. The aggregate may find application in optoelectronic devices.

Acknowledgements

The authors are thankful to IIT Kharagpur, CSIR, UGC and DST New Delhi for financial assistance. We are thankful to Dr P.V. Satyam of IOP, Bhubaneswar for extending help in TEM analysis.

References

1 C. J. Murphy, *Science*, 2002, **298**, 2139.
2 R. D. Kamien, *Science*, 2003, **299**, 1671.
3 (*a*) C. B. Murray, C. R. Kagan and M. G. Bawendi, *Annu. Rev. Mater. Sci.*, 2000, **30**, 545; (*b*) J. H. Fendler, *Chem. Mater.*, 2001, **13**, 3196.
4 (*a*) A. N. Shipway, E. Katz and I. Willner, *ChemPhysChem*, 2000, **1**, 18; (*b*) M. C. Daniel and D. Astruc, *Chem. Rev.*, 2004, **104**, 293.
5 (*a*) C. Petit, A. Taleb and M. P. Pileni, *Adv. Mater.*, 1998, **10**, 259; (*b*) C. B. Murray, C. R. Kagan and M. G. Bawendi, *Science*, 1995, **270**, 1335; (*c*) T. Vossmeyer, G. Reck, L. Katsikas, E. T. K. Haupt, B. Schulz and H. Weller, *Science*, 1995, **267**, 1476.
6 A. Sashchiuk, E. Lifshitz, R. Reisfeld, T. Saraidarov, M. Zelner and A. Willenz, *J. Sol-Gel Sci. Technol.*, 2002, **24**, 31.
7 W. Shenton, D. Pum, U. B. Sleytr and S. Mann, *Nature*, 1997, **389**, 585.
8 R. P. Andres, J. D. Bielefeld, J. I. Henderson, D. B. Janes, V. R. Kolagunta, C. P. Kubiak, W. J. Mahoney and R. G. Osifchin, *Science*, 1996, **273**, 1690.
9 M. Brust, D. Bethell, D. J. Schiffrin and C. J. Kiely, *Adv. Mater.*, 1995, **7**, 795.
10 M. A. Hayat, *Colloidal Gold: Principles, Methods, and Applications*, Academic Press, San Diego, CA, 1989.
11 S. Mann, M. S. Li, S. Connolly and D. Fitzmaurice, *Adv. Mater.*, 2000, **12**, 147.
12 M. Mrksich, *Chem. Soc. Rev.*, 2000, **29**, 267.
13 R. M. Bright, D. G. Waletr, M. D. Musick, M. A. Jackson, K. J. Allison and M. J. Natan, *Langmuir*, 1996, **12**, 810.
14 R. Elghanian, J. J. Storhoff, R. C. Mucic, R. L. Letsinger and C. A. Mirkin, *Science*, 1997, **277**, 1078.
15 U. Kreibig and M. Vollmer, *Optical Properties of Metal Clusters*, Springer, Berlin, 1995.
16 S. Link and M. A. El-Sayed, *J. Phys. Chem. B*, 1999, **103**, 8410.
17 C. A. Mirkin and M. A. Ratner, *Annu. Rev. Phys. Chem.*, 1997, **101**, 1593.
18 M. A. Rampi, O. J. A. Schueller and G. M. Whitesides, *Appl. Phys. Lett.*, 1998, **72**, 1781.
19 D. L. Klein, R. Roth, A. K. L. Lim, A. P. Alivisatos and P. L. McEuen, *Nature*, 1997, **389**, 699.
20 L. A. Bumm, J. J. Arnold, M. T. Cygan, T. D. Dunbar, T. P. Burgin, L. Jones, D. L. Allara, J. M. Tour and P. S. Weiss, *Science*, 1996, **271**, 1705.
21 S. K. Ghosh, S. Kundu, M. Mandal, S. Nath and T. Pal, *J. Nanopart. Res.*, 2003, **5**, 577.
22 J. M. Nam, S. J. Park and C. A. Mirkin, *J. Am. Chem. Soc.*, 2002, **124**, 3820.
23 J. M. Hainfeld and R. D. Powell, *J. Histochem. Cytochem.*, 2000, **48**, 471.
24 L. R. Hirsch, R. J. Stafford, J. A. Bankson, S. R. Sershen, B. Rivera, R. E. Price, J. D. Hazle, N. J. Halas and J. L. West, *Proc. Natl. Acad. Sci. USA*, 2003, **100**, 13549.
25 (*a*) M. Brust, M. Walker, D. Bethel, D. J. Schiffrin and R. Whyman, *J. Chem. Soc., Chem. Commun.*, 1994, 801; (*b*) S. Gao, J. Zhang, Y. Zhu and C. Che, *New J. Chem.*, 2000, **24**, 739; (*c*) S. Nath, S. K. Ghosh, S. Praharaj, S. Panigrahi, S. Basu and T. Pal, *New J. Chem.*, 2005, **29**, 1527.
26 K. V. Sarathy, G. U. Kulkarni and C. N. R. Rao, *Chem. Commun.*, 1997, 537.
27 S. T. Lin, M. T. Franklin and J. K. Klabunde, *Langmuir*, 1986, **2**, 259.
28 (*a*) Y. Nakao, *J. Chem. Soc., Chem. Commun.*, 1994, 2067; (*b*) K. S. Mayya and F. Caruso, *Langmuir*, 2003, **19**, 6987.
29 Y. Dirix, C. Bastiaansen, W. Caseri and P. Smith, *Adv. Mater.*, 1999, **11**, 223.
30 J. I. Kroschwitz and M. Howe-Grant, in *Glass*, 4th edn, ed. J. I. Kroschwitz and M. Howe-Grant, John Wiley & Sons, New York, 1994, **p. 12**569.
31 J. R. Krenn, A. Dereux, J. C. Weeber, E. Bourillot, Y. Lacroute and J. P. Coadonnet, *Phys. Rev. Lett.*, 1999, **82**, 2590.
32 J. B. Pendry, *Science*, 1999, **285**, 1687.
33 E. J. Sanchez, L. Novotny and X. S. Xie, *Phys. Rev. Lett.*, 1999, **82**, 4014.
34 B. Knoll and F. Kellmann, *Nature*, 1999, **399**, 134.
35 T. Wadayama, O. Suzuki, K. Takeuchi, H. Seki, T. Tanabe, Y. Suzuki and A. Hatta, *Appl. Phys. A*, 1999, **69**, 77.
36 P. J. Tarcha, J. Desaja-Gonzalez, S. Rodriguez-Llorente and R. Aroca, *Appl. Spectrosc.*, 1993, **53**, 43.
37 J. J. Storhoff, R. Elghanian, R. C. Mucic, C. A. Mirkin and R. L. Letsinger, *J. Am. Chem. Soc.*, 1998, **120**, 1959.
38 T. Ung, L. M. Liz-Marzán and P. Mulvaney, *J. Phys. Chem. B*, 2001, **105**, 3441.
39 X. Xu, M. Stevens and M. B. Cortie, *Chem. Mater.*, 2004, **16**, 2259.
40 S. Wang, H. Yao, S. Sato and K. Kimura, *J. Am. Chem. Soc.*, 2004, **126**, 7438.
41 A. P. Alivisatos, K. P. Johnsson, X. Peng, T. E. Wilson, C. J. Loweth, M. P. Bruchez Jr and P. G. Schultz, *Nature*, 1996, **382**, 609.
42 Z. Zhong, S. Patskovskyy, P. Bouvrette, J. H. T. Luong and A. Gedanken, *J. Phys. Chem. B*, 2004, **108**, 4046.
43 S. Mandal, A. Gole, N. Lala, R. Gonnade, V. Ganvir and M. Sastry, *Langmuir*, 2001, **17**, 6262.
44 A. Vogel I, *A Text Book of Quantitative Inorganic Analysis*, 4th edn, Longman, London, 1978.
45 W. III. Roy Mason and H. B. Gray, *Inorg. Chem.*, 1968, **7**, 55.
46 K. G. Thomas, J. zajicek and P. V. Kamat, *Langmuir*, 2002, **18**, 3722.
47 U. Kreibig and L. Genzel, *Surf. Sci.*, 1985, **156**, 678.
48 S. Tsakiris, K. H. Schulpis, K. Marinou and P. Behrakis, *Pharmacol. Res.*, 2004, **49**, 475.
49 M. Barbagallo, L. J. Dominguez, M. R. Tagliamonte, L. M. Resnick and G. Paolisso, *Hypertension*, 1999, **34**, 1002.
50 T. Yamaguchi, I. Katoh and S. Kurata, *Eur. J. Biochem.*, 2002, **269**, 2782.
51 G. K. Balendiran, R. Dabur and D. Fraser, *Cell Biochem. Funct.*, 2004, **22**, 343.
52 K. Takehara and Y. Ide, *Bioelectrochem. Bioenerg.*, 1992, **29**, 103.
53 S. G. Tajc, B. S. Tolbert, R. Basavappa and B. L. Miller, *J. Am. Chem. Soc.*, 2004, **126**, 10508.
54 S. B. Lee, K. Kim and M. S. Kim, *J. Raman Spectrosc.*, 1991, **22**, 811.
55 J. Isrealachvili, *Intermolecular and Surface Forces*, 2nd edn, Academic Press, San Diego, CA, 1992.